(10)

THE UNIVERSITY OF TEXAS

Austin 12

Contract Nonr-375(05)

Task No. NR 051-381

Final Report

Relaxation Processes in Liquids and Solids

A. W. Nolle, Chief Investigator
Department of Physics

1 April 1960

Final Report

Contract Nonr-375
Task No. NR 051-381

Outline

A. High Polymers
   1. Magnetic Resonance in Polyisobutylene at Various Pressures and Temperatures
   2. Magnetic Resonance of Polymer Solutions
   3. Longitudinal Waves in Polymers under Pressure
   4. Transverse Ultrasonic Waves in Polyisobutylene under Pressure

B. Dielectric Liquids
   5. Nuclear Magnetic Resonance in Degassed Organic Liquids under Pressure
   6. Effect of Pressure on Ultrasonic Absorption in Non-Associated Liquids
   7. Ultrasonic Relaxation in 2,2 Dimethylbutane
   8. Ultrasonic-Wave Study of Liquid Crystal Compounds
   9. Magnetic Resonance Investigation of Liquid Crystal Compounds

C. Paramagnetic Solutions
   10. Frequency Dependence of Proton Spin Relaxation Times
   11. Electron Paramagnetic Resonance in Solutions Containing Paramagnetic Ions
   12. Electron Paramagnetic Resonance in Frozen Solutions

D. Crystalline Solids
   13. Magnetic Resonance Investigation of Molecular Motion in 2,2-Dinitropropane
   14. Spin-Lattice Relaxation Time in Ionic Crystals at Elevated Temperatures

E. Special Topics in Apparatus and Methods
   15. Marginal Oscillator NMR Detector with Frequency Control
   16. Apparatus for Longitudinal Wave Transmission in High Polymers under Pressure
   17. Spin-Echo Pulsing Equipment
   18. Equipment for Direct Measurement of T_1

THE UNIVERSITY OF TEXAS

Austin 12

Contract Nonr-375(05)
Task No. NR 051-381

Final Report

This report summarizes research work done in the period 1 February 1954 - 31 January 1960, under the general theme of relaxation processes in liquids and solids. The experimental work has consisted mainly of investigations of magnetic resonance relaxation, with a slightly smaller quantity of work on relaxation processes in ultrasonic-wave absorption. The results have lead to information concerning thermally activated molecular processes in high polymers, in molecular liquids, in aqueous solutions with paramagnetic ions, and in crystalline solids. In the discussion which follows, it is convenient to follow this classification in terms of the systems investigated, and to reserve a concluding section of the report for miscellaneous topics concerning apparatus and procedures.

A. High Polymers

1. Magnetic Resonance in Polyisobutylene at Various Pressures and Temperatures

(Reference: "Proton Magnetic Resonance in Polyisobutylene at Various Temperatures, Pressures, and Frequencies", A. W. Nolle and J. J. Billings, J. Chem. Phys. 30, 84 (1959.)

This investigation concerned both the line width and the relaxation time for proton magnetic resonance in polyisobutylene of molecular weight 1.35×10^6. The line width was measured at temperatures between -100°C and 32°C, in a pressure range from atmospheric pressure to 1060 kg/cm^2, with the results shown in Fig. 1. A steady-state method was used, at 28.8 mc. By graphical analysis of the data, it was found that the derivative dT/dp for constant line width, which may be thought of as the temperature increase required to compensate the effect of a unit increase of pressure, is 0.023 C°/atm, except that a somewhat greater initial value is found for pressures under 200 atm. It will be shown that other pressure-temperature experiments on polymers give comparable values. Since the magnetic resonance behavior of polyisobutylene is determined largely by the magnetic coupling between hydrogen nuclei in the same molecular chain, (J. G. Powles, Proc. Phys. Soc. (London) B69, 281 (1956)), it follows that the important effect of applying pressure is to modify the thermal motions affecting short portions of a chain. The derivative dT/dp described above is therefore a derivative for constant jump rate with regard to these motions.

The spin-lattice relaxation time, T_1, was measured by transient methods. At 28.8 mc, T_1 was found to increase in nearly linear fashion with pressure. The ratio of T_1 at 1060 kg/cm^2 pressure to the value at atmospheric pressure was found to be 1.40, 1.20, and

1.06, for temperatures of 30°, 50°, and 65°C, respectively. The small effect of pressure at 65° is to be expected from the measurements by Powles and Luszczynski on T_1 vs. temperature at atmospheric pressure, from which it may be deduced that at the present measuring frequency, T_1 passes through a minimum at approximately 65°C.

Further measurements were made of T_1 as a function of frequency, at 26°C and atmospheric pressure, as shown in Fig. 2. It is seen that the dependence of T_1 on frequency is approximately linear, instead of following the function which is calculated by the use of one correlation time in the well known BPP theory (Bloembergen, Purcell, and Pound, Phys. Rev. 73, 679 (1948)). The inference is that the spin-spin interactions are affected by a distribution of correlation times. In principle, this distribution could be obtained by analysis of the T_1 vs. frequency function, but in practice, the experimentally available range of frequencies covers somewhat less than two decades, which is not sufficient. It is of course possible that the effect of a wider frequency coverage could be obtained by varying both temperature and frequency, provided that the reduced-variables principle, which has been used in the dynamic viscoelastic behavior of polymers, is applicable. This has not been tried.

The problem of a distribution of correlation times was considered also in connection with the line-width data. Analysis of the atmospheric pressure curve for line width as a function of temperature, by well known methods (H. S. Gutowsky and G. E. Pake, J. Chem. Phys. 18, 162 (1950)), indicates that the chain motions determining the line width have an activation energy of about 4 kcal/mole. This is in conflict with the results of viscoelastic measurements, from which a value of the order of 20 kcal/mole has been found (Ferry,

Grandine, and Fitzgerald, J. Appl. Phys. 24, 911 (1953)). In the publication cited under the heading of this section, a possible explanation of this difficulty was obtained by computing, on the basis of the general procedures in the BPP theory, the behavior of the line width in the case of a continuous distribution of correlation times. It was found, for example, that an attempt to obtain an energy of activation from the line width vs. temperature data for the case of a box-plus-wedge distribution would ordinarily yield answers less than half the correct value, depending upon the part of the line-width data chosen for analysis. The "correct value" here means a single activation energy which was assumed to apply for motions having all allowed values of correlation time.

2. Magnetic Resonance of Polymer Solutions

(References: Technical Report No. 1, July 1955; abstract in Phys. Rev. 98, 1560 (1955); abstract in Bull. Am. Phys. Soc. II 1, 109 (1956).)

The magnetic resonance investigation of polymer solutions in this program has utilized the hydrogen nuclear resonance exclusively, and has been restricted largely to the case in which the solvent has negligible magnetic susceptibility and contains no hydrogen. Because the magnetic interactions between hydrogen nuclei affect the absorption line width and the relaxation rate (the reciprocal of T_1) inversely as the sixth power of the distance of separation, interactions between remote parts of the polymer chain, or between different chains, make no appreciable contributions to these quantities in the case of a solution. Thus, the NMR study of solutions gives, primarily, information concerning the thermal motion of individual chain segments or side groups. It will be seen that the segmental motion shows intermolecular effects when

the solution is not sufficiently dilute, however.

All NMR measurements on solutions utilized the two- or three-pulse spin-echo techniques of Hahn (E. L. Hahn, Phy. Rev. 80, 580 (1950)), which show the time dependence of the longitudinal magnetization (in the direction of the field of the laboratory magnet) and of the transverse magnetization when the sample has been disturbed from equilibrium. In the simplest case, these time dependences are exponential, and lead to the longitudinal or spin-lattice relaxalion time, T_1, and the transverse relaxation time, T_2, respectively. The time functions observed here were exponentials within experimental error, so that this interpretation was used. It should be pointed out that the signal-to-noise ratio is relatively poor in solution work, so that it would not have been possible to detect small admixtures of additional exponential terms. It is useful to recall that the width of the absorption line in cycles per sec is $(\pi T_2)^{-1}$, for a Lorentzian line shape. The experimental frequency was 28.8 mc, unless otherwise specified.

Figure 3 shows the relaxation times, T_1 and T_2, as functions of concentration, for polyisobutylene of viscosity average molecular weight 1.35×10^6, in CCl_4. The experimental results reproduce to within about 5% at the higher concentrations. The smallest concentration gave a barely useful signal to noise ratio. For the small concentrations, the data points are averages of many runs with individual uncertainties of about 20%.

The outstanding feature of the results in Fig. 3 is the well-defined knee, marking the upper limit of a dilute-solution region in which T_1 and T_2 are independent of concentration. Corresponding dilute-solution effects have been found by other investigators by

viscosity measurements and by ultrasonic absorption measurements. A simple explanation, in good agreement with the facts, is that the knee occurs at the concentration where appreciable entangling occurs between adjacent polymer balls in the solution. As an approximation, the average spacing between molecular centers, a, obeys the relation

$$W = M/Aa^3$$

where W is the concentration in gm/cm^3, M is the molecular weight, and A is Avogadro's number. A relation due to Flory (P. J. Flory, J. Chem. Phys. 17, 303 (1949)) gives the radius of the polymer ball as

$$R = 0.52 \alpha l Z^{1/2}$$

where α is an excluded volume correction factor, which is unity in the case where the finite segmental volume is neglected, l is the length of a segment in the equivalent chain, and Z the total number of links. Use of these two relations, with α equal to unity, gives a calculated value of 0.03 gm/cm^3 in fair agreement with the experimental value of 0.05 gm/cm^3, in view of the approximations.

It may be inquired how T_1 and T_2 are reduced in the solutions having concentrations just above the knee, if the overlap of adjacent polymer balls is (statistically) slight, and affects only a fraction of the chain segments. The answer is that magnetic mixing must be taking place in a time short compared to T_1 and T_2, or single relaxation times would no longer be observed. This can occur through statistical fluctuations in the configuration of the molecule, so that in a time short compared to T_1 and T_2, various segments appear at the periphery, and through spin-spin diffusion, which occurs rapidly when the line width is relatively large, as it is here.

The absolute value of T_1 in the dilute solution region, from Fig. 3, gives the correlation time for segmental rotation as 1 to 2 times 10^{-9} sec, on the basis of the BPP theory. The same theory, with a correction for the fact that the elastic stiffness of the chain varies as T, the absolute temperature, predicts that T_1 or T_2 should vary approximately as η/T^2, where η is the viscosity coefficient. This was verified with T_2 measurements from 0°C to 70°C, for the polyisobutylene used for the data of Fig. 3. Both a concentrated solution and a dilute solution were used. This indicates, additionally, that the correlation times for segmental rotation vary approximately as η/T^2.

Further information was obtained by making sets of measurements as in Fig. 3 for polyisobutylenes of various molecular weights. The explanation given above for the knee of the relaxation time vs. concentration curves may be used to predict that the critical concentration should vary as the -1/2 power of the molecular weight. This relation was found to hold true approximately on the basis of T_2 curves for four samples of molecular weights 75,000 to 2×10^6, but not for two samples of molecular weight below 10,000, for which sharp knees were not found in the T_2 curves.

On the grounds that T_1 and T_2 are controlled by segmental rotations, the values found for these quantities in dilute solution are expected to be unaffected by reduction of molecular weight, until finally, at sufficiently small molecular weight, the segmental jump frequency begins to rise toward that for a liquid of low molecular weight, which is some 100 times faster, and according to the BPP theory, to bring about an increase of T_1. This was verified by the measurements. The relaxation times for dilute solutions showed no

systematic variation with molecular weight from 2 x 10^6 down to 10^4, but an increase of T_1 was found in a sample of molecular weight about 2000. (The fact that T_2 had not yet been begun to rise with this amount of reduction in molecular weight suggests that the theory for a single correlation time does not apply strictly.)

The effect of varying the solvent viscosity, without varying the temperature, was studied by measuring the NMR relaxation times for polyisobutylene solutions as a function of pressure. The viscosity of the solvent, CCl_4, as a function of pressure, is known from the work of Bridgman. The relaxation times decrease by a factor of 2 with 1000 atmospheres pressure. This is somewhat less than the factor by which the viscosity changes. The deviation is in the expected direction, for the correlation time mentioned earlier for segmental rotation, 10^{-9} sec, corresponds nearly to the minimum in the function giving T_1 as a function of correlation time in the BPP theory. The relaxation times in this region vary less rapidly than the first power of the correlation time, and therefore, less rapidly than the first power of the viscosity. A more thorough analysis remains to be made.

Generally similar results to those for polyisobutylene solutions were obtained for CCl_4 solutions of polystyrene, for which the relaxation times are about one-third of those obtained with polyisobutylene.

3. Longitudinal Waves in Polymers under Pressure

(Reference: "Pressure Dependence of the Viscoelastic Behavior of Polyisobutylene", Harkrishan Singh and A. W. Nolle, J. Appl. Phys. 30, 337 (1959).)

In Section 1, conclusions were reached about the relative effects of temperature and pressure on the segmental jump rate in

polyisobutylene from NMR line width data. Another approach which also gives the relative effects of temperature and pressure on the jump rate is to observe the relative effects of these variables on the dynamic mechanical properties. This was done by use of an ultrasonic-wave method, as described below. The experimental quantities discussed will be the velocity and absorption coefficient for longitudinal waves. These are determined by the dynamic shear compliance and the dynamic bulk compliance, but it is not possible to evaluate these compliances from longitudinal-wave data only.

The experiment is based on a method used earlier for measurements at atmospheric pressure (A. W. Nolle and S. C. Mowry, J. Acous. Soc. Am. 20, 432 (1948)). The phase velocity and absorption coefficient for longitudinal waves in a thin lamina of the polymer are calculated from the changes which occur in the amplitude and travel time of signals propagated in a liquid path in a pulse-reflection apparatus, when the sample is inserted in the path. For the present measurements, a magnetically actuated device was built (Sec. 16) to move the sample into and out of the ultrasonic signal path in a closed pressure vessel.

The interpretation of the data will be based on the behavior of the absorption, which proved to allow of more accurate measurement than the phase velocity. At each constant pressure, the absorption passes through a maximum (which is somewhat in excess of 100 db/cm at a measuring frequency of 4 mc) with variation of the temperature. A family of these constant-pressure absorption curves was prepared. The temperatures of the absorption maximum for various pressures up to 1500 atmospheres are as shown in Fig. 4. An additional data point for atmospheric pressure was taken from Marvin, Aldrich, and

Sack (J. Appl. Phys. 25, 1213 (1954)). The straight line which best fits the data (not shown) has a slope of 0.019 C^{o}/atm, comparable in magnitude to the value of 0.023C^{o}/atm for constant jump rate as found from the NMR data (Sec. 1).

The straight line drawn in Fig. 4, which is not a bad representation of the data, has a slope of 0.025 C^{o}/atm. This was computed by adapting a theory due to Bueche (F. Bueche, J. Chem. Phys. 21, 1850 (1953)), in which the segmental jump rate is taken to be a function of an effective volume. The effective volume is connected with an effective thermal expansion coefficient which is the difference between the total expansion coefficient and that observed at temperatures below the glass transition. It should be stressed that the agreement found here with the Bueche theory is better than the accuracy with which the quantities which go into the calculation are known.

To interpret the ultrasonic measurements, it was necessary to know the volume-pressure function for polyisobutylene. This was found, for pressures up to 1500 atm, with a specially built dilatometer having a series of electrical contacts on the capillary.

The longitudinal-wave measurements were performed also for a vulcanized sample of Buna-N rubber. The shifting factor dT/dp does not differ significantly from that for polyisobutylene.

A limitation of the experimental method is that the polymer sample is in contact with a liquid. Ethyl alcohol produces linear swelling of no more than 2% in polyisobutylene for the range of temperatures in which the absorption peak was found and less for the Buna-N vulcanizate, but it is to be expected that sufficiently accurate measurements would show that the ultrasonic-wave propagation

constants found here are different from those from samples from which liquid is excluded.

4. Transverse Ultrasonic Waves in Polyisobutylene under Pressure

A desirable corollary to the preceding investigation with longitudinal ultrasonic waves would be an investigation using transverse waves. If both sets of measurements could be done with sufficient accuracy, the complex dynamic compliances for compression and for shear could be computed from the combined results. The experiment to be described here ran into difficulty short of this goal, but did lead to a value of dT/dp for constant segmental jump rate which is based on behavior in shear only.

The transverse-wave experiment was intended to carry out under pressure a measurement procedure which had been used earlier at atmospheric pressure (A. W. Nolle and P. W. Sieck, J. Appl. Phys. 23, 888 (1952)). In this method, pulsed ultrasonic signals are conducted through solid, cylindrical delay lines separated by a laminar polymer sample, which is bonded to the proximate end surfaces of the cylinders. The signals are generated and received by Y-cut, resonant quartz plates. In the present case, special delay lines were fabricated from Y-cut quartz, in order that the source and detector quartz disks could be soldered to these and remain connected without being affected by differential expansion. The present sample, polyisobutylene of molecular weight 1.35×10^6, bonded well to the quartz delay lines when heated to about 130°C; no cement was necessary.

As a sample less than 2 mm thick had to be used to transmit a useful signal in the 10° - 20°C range, absolute measurements

of the phase velocity were not attempted, but instead the change in phase of the transmitted signal under pressure was observed, to permit computation of the change in phase velocity. Absolute values for both phase velocity and absorption were obtained at atmospheric pressure by calculation from the FGF reduced-variables curves (Ferry, Grandine, and Fitzgerald, J. Appl. Phys. 24, 911 (1953)).

The results are shown in Fig. 5, where part A shows the values at atmospheric pressure calculated from the FGF data for a frequency of 2 mc, at which the measurements were performed, and where part B shows the effects of pressure, from the present measurements. The absorption was successfully measured at 10°C, and the phase velocity variation at 20°C.

Comparison of parts A and B in the figure gives an averaged value of dT/dp for constant jump rate (in this case, constant wave propagation constants) of 0.013 C°/atm. This probably does not represent a significant deviation from the value of 0.019 C°/atm from the longitudinal-wave experiments above. The result shows that the processes connected with compressional and with shear distortion of the polymer, at high frequencies, have very nearly the same volume of activation, and may well represent the same basic activation phenomenon.

The experiment had to be terminated when the soldered quartz crystal joints deteriorated because of electrolytic attack under pressure by the fluid medium, which was ethyl alcohol. The results have been described in a letter submitted to the Journal of Applied Physics.

B. Dielectric Liquids

5. Nuclear Magnetic Resonance in Degassed Organic Liquids under Pressure

(Reference: "Effects of Pressure on Proton Spin-Lattice Relaxation in Several Organic Liquids" (abstract), A. W. Nolle and P. P. Mahendroo, Bull. Am. Phys. Soc. II 4, 170 (1959).) (In pub., J. Chem. Phys.)

The effect of pressure on the spin-lattice relaxation time, T_1, was investigated for several dielectric liquids by Benedek and Purcell (G. B. Benedek and E. M. Purcell, J. Chem. Phys. 22, 2003 (1954)). For those liquids where data were available for comparison, it was found that under pressure, T_1 decreased more rapidly than the fluidity or the self-diffusion coefficient. On the basis of the BPP theory, it was concluded from this that the jump rate for molecular translational processes is slowed more, under pressure, than that for rotation. Excepting the case of water, the samples used in the study were not degassed.

Later, it was shown that the removal of dissolved gases gives an increase of T_1 in these liquids. For aromatic compounds, this amounts to several hundred per cent. For the aromatic compounds, then, the result of Benedek and Purcell actually showed that pressure was more effective in slowing molecular translation than in slowing the diffusion jump rate of dissolved O_2, for the latter process actually controlled T_1. Accordingly, the investigation described below was undertaken, to determine whether the original conclusion needed to be revised for degassed liquids.

The relaxation times were measured by a pulse method, at 28.8 mc, in degassed samples of toluene, benzene, cyclohexane, methyl iodide, 1,1,1-trichloroethane, and n-heptane. Chloroform was examined, but was not successfully degassed. Degassing was done by a cycle of

freezing, pumping, and thawing, which usually was repeated several times. The special cartridge used to hold the specimen liquids in the pressure chamber is shown in Fig. 6. The surrounding pressure fluid was Kel-F No. 10 oil, a fluorocarbon which contributes no hydrogen NMR signal. The mercury seal was effective in preventing contamination of the sample by the pressure fluid.

For liquids in which degassing causes a relatively small increase in T_1 (e.g., methyl iodide and n-heptane, in which the increase is less than 20%), the plot of normalized T_1 vs. pressure did not differ greatly from that of Benedek and Purcell, and there was no reason to alter the conclusion expressed by them, that rotational processes were less affected than translational processes under pressure. For toluene and benzene, however, the behavior of the degassed samples was entirely different from that without degassing. The effect of pressure on the normalized T_1 became comparable to that on the fluidity. In benzene, the normalized T_1 is initially more sensitive to pressure than is the fluidity, as shown in Fig. 7. Corresponding results for toluene are shown in Fig. 8. The viscosity data used in both figures are from the papers of P. W. Bridgman.

A calculation based on the specific volume shows that a large part of the sharp initial decrease of T_1 in benzene may be due to reduction of the intermolecular hydrogen-hydrogen distances.

For toluene and benzene, then, the conclusion from the new data is that the effects of pressure in slowing translational and rotational jump processes are comparable in magnitude. There is of course no evidence that the effects are identical.

6. Effect of Pressure on Ultrasonic Absorption in Non-Associated Liquids

(Reference: "Velocity and Absorption of Ultrasonic Waves in Several Non-Associated Liquids under High Pressure", J. F. Mifsud and A. W. Nolle, J. Acous. Soc. Am. 28, 469 (1956).)

The velocity and absorption of ultrasonic waves were measured under pressures up to 1360 atm in carbon tetrachloride, benzene, and carbon disulfide, at frequencies in the range 2 - 10 mc. These are liquids for which the absorption is many times as great as that which can be attributed to the shear viscosity. Qualitatively similar results were found for the three liquids. At the maximum pressure, the absorption is about 0.4 of the value at one atmosphere, and the propagation velocity is about 1.4 times the initial value.

Explanations of the absorption were considered on the basis of (1) structural relaxation, in which a delayed molecular rearrangement occurs to reduce the volume in response to the acoustical pressure, and (2) thermal relaxation, in which energy is not conserved because of a time lag in excitation of internal molecular motions which contribute to the equilibrium specific heat. Several aspects of the available information, including the present measurements, rule out (1), but thermodynamic data for the liquids under pressure are not accurately enough known to allow more than a rough evaluation of (2), which however must be regarded as the likely explanation.

This piece of work was almost completed at the commencement of the research contract with which this report is concerned. The completion of this work paved the way for the other pressure studies which are reported.

7. Ultrasonic Relaxation in 2,2 Dimethylbutane

(Reference: "On Sound Absorption in Liquids Having Rotational Isomerism"; (abstract), A. W. Nolle and J. D. Payne, J. Acous. Soc. Am. 29, 180 (1957).)

The foregoing work dealt with the effects of pressure on sound absorption which was apparently due to thermal relaxation. The discovery by Petrauskas and others of large absorption in 2,2 dimethylbutane and other compounds having rotational isomerism suggested that there might be a possibility here of studying absorption due to structural relaxation, the specific mechanism being a retarded change in volume under acoustic pressure as the transition from one isomeric configuration to the other is promoted. Accordingly, velocity and absorption in 2,2 dimethyl-butane were measured at frequencies between 4 and 31 mc, in a temperature range -35°C to 25°C, and a pressure range up to 1500 kg/cm^2. The data were processed to determine the parameters which, when used in structural relaxation theory, would most nearly explain the results. It was necessary to use a relaxing volume of about 40% of the total liquid volume. This is unreasonably large for the isomeric change, and makes it doubtful that the theory of structural absorption applies. Other investigators showed that the effect of pressure on the relaxation times is consistent with thermal absorption.

8. Ultrasonic-Wave Study of Liquid Crystal Compounds

(Reference: "Behavior of Liquid-Crystal Compounds Near the Isotropic-Anisotropic Transition", W. A. Hoyer and A. W. Nolle, J. Chem. Phys. 24, 803 (1956).)

The object of this investigation was to examine in fine detail the behavior of the ultrasonic-wave absorption coefficient and the

velocity in the phase transition regions of liquid crystal compounds, and to analyze the data in terms of the theory of heterophase fluctuations. The compounds were p-azoxyanisole and cholesterol benzoate, which have liquid-crystal phase transitions at approximately 136°C and 177°C respectively. A specially constructed temperature system was used, which included an unstirred inner bath, almost completely surrounding the sample chamber, and a vigorously stirred outer bath, regulated to about $\pm$ 0.005°C. The sample was maintained in a nitrogen atmosphere.

Typical results appear in Fig. 9, where it is shown (for p-azoxyanisole) that the ultrasonic absorption has a very sharp maximum at the transition, and that the velocity has a minimum, which is the beginning of a sudden rise which leads to the higher value in the isotropic (higher temperature) phase. Such measurements were carried out from 0.5 mc to 6.0 mc.

The interpretation is considered at length in the published paper. The variation of the compressibility with temperature in the transition region is explained fairly well by the heterophase fluctuation theory of Frenkel, which pictures the material, near the transition, as a medium in which there exist aggregates of molecules in the other phase, the aggregates containing an increasing quantity of the material as the transition is approached. The ultrasonic absorption in the transition region has a frequency dependence which indicates a relaxation time of about 10^{-8} sec, the exact value varying with temperature. The magnitude of the ultrasonic absorption is well accounted for by structural relaxation theory in which the pretransitional increment in the compressibility is considered to "relax".

9. Magnetic Resonance Investigation of Liquid Crystal Compounds

(Reference: "Nuclear Magnetic Resonance Study of Liquid Crystal Compounds", W. R. Runyan and A. W. Nolle, J. Chem. Phys. 27, 1081 (1957).)

This investigation was undertaken to examine the following questions: (1) Does the amplitude of the magnetic resonance signal component of the normal liquid (long T_1) vary with temperature in the transition region in agreement with the predictions of heterophase fluctuation theory concerning the quantity of normal liquid which is present? (2) Are the values of the magnetic resonance relaxation times in the isotropic liquid phase consistent with those in liquids which do not form liquid crystal phases? (3) Do relaxation times change with approach to the transition in a way consistent with the heterophase fluctuation theory? In connection with these questions, it should be borne in mind that it had already been shown by other investigators (Jain, Lee, and Spence, J. Chem. Phys. 21, 1891 (1953)) that the anisotropic phase gives a structured absorption curve covering about 4 oersteds (which is consistent with a picture of axially parallel molecular groups in the anisotropic phase), and that the signals due to this phase would consequently last for too short a time to be observed in the spin echo apparatus which was used in the present work.

Regarding point (1), the experiment did not yield the desired results. It was found that the anisotropic-isotropic transition could not be induced simultaneously in all parts of a sample vial, but that an interface sweeps gradually through the sample. This apparently produces a zone refining operation, while at the same time

slow thermal decomposition of the sample occurs. These effects cause the amplitude of the NMR signal in the transition region to depend in a complicated fashion on the history of the sample, and prevented use of the amplitude data as a test of heterophase fluctuation theory.

As regards point (2), the relaxation times in the case of the isotropic liquids were consistent with those in comparable liquids which do not form a liquid crystal phase, which tends to confirm the view that the phase change in question does lead to a normal liquid.

In connection with the third objective, a decrease in the spin-lattice relaxation time for the isotropic phase of p-azoxyanisole was observed as the temperature was lowered toward the transition, as shown in Fig. 10. This is the pretransitional effect to be expected from heterophase fluctuation theory, the formation of larger aggregates serving to introduce slower thermal motions, which in the case of this liquid leads to a greater relaxation time. Pretransitional decreases in the transverse relaxation time, T_2, were found in the cholesterol derivatives included in the study (cholesteryl benzoate, n-butyrate, and propionate). Because of excessive diffusion, T_2 measurements were not obtained for p-azoxyanisole.

While the behavior of the relaxation times is qualitatively consistent with the heterophase fluctuation theory, the preceding ultrasonic investigation is a more extensive and more precise indication of pretransitional effects.

C. Paramagnetic Solutions

10. Frequency Dependence of Proton Spin Relaxation Times

(References: "Frequency Dependence of Proton Spin Relaxation in Aqueous Solutions of Paramagnetic Ions", A. W. Nolle and L. O. Morgan, J. Chem. Phys. 26, 642 (1957).
"Proton Spin Relaxation in Aqueous Solutions of Paramagnetic Ions, II, Cr^{+++}, Mn^{++}, Ni^{++}, and Gd^{+++}", L. O. Morgan and A. W. Nolle, J. Chem. Phys. 31, 365 (1959).)

The first reference concerns the NMR relaxation times of aqueous solutions containing Cr^{+++}, Mn^{++}, Co^{++}, and Nd^{++}, at room temperature, for various frequencies from 2.7 to 28.7 mc. The two and three pulse spin echo techniques of Hahn were used. In each case, it was established that the relaxation times (T_1 and T_2) are inversely proportional to concentration for dilute solutions. Data were therefore reduced to products NT_1, NT_2, where N is the molar concentration. The most striking result was a frequency dependence of the relaxation times for Cr^{+++} and for Mn^{++}, shown in Fig. 11.

It was shown by an application of the BPP analysis that such increases of relaxation time with experimental frequency can be anticipated whenever ω, the radian frequency, is of the order of $1/\tau$, where τ is the correlation time of a random process affecting the time dependence of the magnetic energy of the hydrogen nuclei. Such processes might be the exchange of hydrogen nuclei between the bulk of the liquid and the hydration sphere of the paramagnetic ion, or the random tumbling of the complex. In a dispersion region, $1/T_1$ will have a component varying as $(1+\omega^2\tau^2)^{-1}$. Fitting the results in Fig. 11 to this function gave values of τ of 7.6×10^{-9} sec for Cr^{+++} and 8.8×10^{-9} sec for Mn^{++}.

These times were not implausible for exchange in the hydration sphere, but it was noted that exchange times of the above values should give much smaller values of T_1, if the exchange involves water at the minimum distance from the ion. The behavior of T_2 was also discussed. Only a minor dispersion effect is predicted in T_2, so that T_1/T_2 increases with frequency in the dispersion range, as shown in Fig. 11.

A better analysis of the problem became possible with the publication by Solomon of a rigorous treatment of relaxation involving two isolated spins (I. Solomon, Phys. Rev. 99, 559 (1955)). It was pointed out by Bloembergen and Codrington that additional terms should be included on account of the scalar spin-spin interaction (R. S. Codrington and N. Bloembergen, J. Chem. Phys. 29, 600 (1958)). When this is done, and when justifiable approximations are made, there follows

$$(NT_1)^{-1} = (4/30)\left[S(S+1)g^2\beta^2\gamma_I^2 p' r^{-6}\right]\left[3\tau_c + 7\tau_c(1+\omega_s^2\tau_c^2)^{-1}\right]$$
$$+ (2/3)\left[S(S+1)A^2 p' \hbar^{-2}\right]\left[\tau_e(1+\omega_s^2\tau_e^2)^{-1}\right]$$

$$(NT_2)^{-2} = (4/60)\left[S(S+1)g^2\beta^2\gamma_I^2 p' r^{-6}\right]\left[7\tau_c + 13\tau_c(1+\omega_s^2\tau_c^2)^{-1}\right]$$
$$+ (1/3)\left[S(S+1)A^2 p' \hbar^{-2}\right]\left[\tau_e + \tau_e(1+\omega_s^2\tau_e^2)^{-1}\right]$$

where p' is the probability that a proton occupies a position in a hydration sphere of a paramagnetic ion in a 1M solution of the ions, and the other symbols in the multiplicative constants are conventional. Some important features of the equations are as follows:

1. The observed dispersion in T_1 occurs when $\omega_s\tau_c \simeq 1$, where ω_s is the electron processional frequency and τ_c the correlation

time for the dipolar interaction with a proton in the hydration layer. This differs from the first interpretation, in which the possibility that the dispersion has only to do with the proton precessional frequency was considered.

2. If the isotropic spin-spin interaction, of magnitude A, is large, and the accompanying correlation time, τ_e, is sufficiently small, no frequency dependence of the T_2 for proton resonance is observable.

3. The ratio of T_1 for high frequencies to the value for low frequencies is 10/3.

4. Dispersion effects dependent on the value of the proton precessional frequency (ω_I) are predicted in the full theory, but do not appear in the approximations above, where it is assumed that these occur at frequencies well above the experimental range.

This improved theory explains the magnitudes of the relaxation times with reasonable values of the hydration sphere radius, on the basis of $\tau_c \approx 10^{-11}$ sec, the latter value coming directly from the experimentally observed frequency dependence. Apparently τ_c is the correlation time for tumbling of the complex. In investigations from 1.9 to 60 mc reported in the second reference, dispersion ranges were observed for Cr^{+++}, Mn^{++}, Cu^{++}, and Gd^{+++}, but none showed the full 10/3 effect. This remains a problem for investigation. Variation of τ_e seems to be important.

11. Electron Paramagnetic Resonance in Solutions Containing Paramagnetic Ions

Electron paramagnetic resonance has been observed at approximately 9 kmc for solutions containing Cu^{++} and Cr^{+++} ions and complexes. These have included various concentration ratios in the systems Cu-ethylenediamine and Cu-bipyridyl in aqueous solution. These two systems show the copper hyperfine structure, which is not displayed in aqueous solution. Apart from its intrinsic interest, this problem was taken up as an extension of the preceding topic, the electron resonance method giving an alternative way of investigating spin-spin interactions, tumbling correlation times, and electronic relaxation times. The latter determine τ_e in one limiting case.

This work is continuing. The results have not yet been reduced for publication.

12. Electron Paramagnetic Resonance in Frozen Solutions

(Reference: "Paramagnetic Resonance of Mn^{++} Ions in Ice" (Abstract), Fahd Wakim and A. W. Nolle, Bull. Am. Phys. Soc. II 2, 111 (1960).

Electron paramagnetic resonance in aqueous solutions can be further understood if the limiting case of negligible tumbling motion is investigated, through the use of quick-frozen solutions. The absorption lines have been observed for frozen solutions with Mn^{++} and Cu^{++} ions, and for the copper complex systems mentioned in the preceding section. The spin-lattice relaxation times have not yet been measured.

The hyperfine structure is resolved in frozen solutions of

the Cu^{++} complexes, but single broad lines are obtained from frozen aqueous solutions with Cu^{++} or Mn^{++} ions.

The explanation of the Mn^{++} absorption curve, which has a slope width of 760 oe, has been considered. It is assumed that the ion is in a distorted tetrahedron formed by six water molecules. The single-crystal absorption spectrum for this configuration is well known (B. Bleaney and D. J. E. Ingram, Proc. Roy. Soc. A 205, 336 (1951)), and consists of 30 lines with characteristic angular dependences. Space-averaging this specturm gives an approximation to a single broad line. The width of 760 oe for the Mn-ice system is explained if the constant D of the spin Hamiltonian, which is an index of the departure from a cubic arrangement, is approximately twice the value found by Bleaney and Ingram for the Mn^{++} ion in manganese fluosilicate, where it is surrounded by a tetragonal arrangement of six H_2O molecules.

D. Crystalline Solids

13. Magnetic Resonance Investigation of Molecular Motion in 2,2-Dinitropropane

(Reference: "Investigation by Nuclear Magnetic Resonance of the Effects of Pressure on the Thermal Transition and Rotator Phase of 2,2-Dinitropropane", J. J. Billings and A. W. Nolle, J. Chem. Phys. 29, 214 (1958).)

At $-5^{\circ}C$, there exists a transition in the dielectric behavior of 2,2-dinitropropane and in the NMR line width, which has been assumed to mark the onset of free rotation. The present investigation was undertaken to determine the nature of the transition (whether first or second order) and to determine more particularly the onset of molecular rotation and diffusion in the transition region as pressure and temperature are varied. The NMR line width was

determined as a function of temperature and pressure, by conventional slow-passage absorption measurements, at 28.8 mc. The spin-lattice relaxation time was determined by transient techniques. Thermal expansion of the sample in the transition region was observed with a precision dilatometer. The compressibility was measured on each side of the transition, and finally, X-ray structural examinations were made, also both above and below the transition temperature.

The rapid decrease of NMR line width with increasing temperature in the phase transition region is reproduced (very nearly) at higher temperatures when pressure is applied. A family of curves showing this at various constant pressures appears in Fig. 12. The value of T_1 increases almost by a factor of 10 with transition to the rotator phase, as shown in Fig. 13. At atmospheric pressure, T_1 rises continuously as the temperature is increased to the melting point, but under 1000 kg/cm^2 pressure, it is found that there is a broad range in the rotator phase where T_1 is independent of temperature.

The thermal expansion measurements and the X-ray results are reported in the reference. The cubic lattice constant changes from 8.86 ± 0.07A in the rotator phase to 17.8 ± 0.1A in the phase below the transition.

The details of the discussion will be omitted from this summary. Among the conclusions reached are the following:

1. The ratio of applied pressure to increase of transition temperature is 60 atm/C°. From this, and from the volume-temperature relationships found near the transition, the heat of transition is found to be 2.92 kcal/mol. The transitional increase in heat capacity is $\Delta C_p = 26.5$ cal/C° mole. All of these numerical

values are comparable to corresponding ones for known first-order transitions.

2. The X-ray evidence is consistent with a first-order transition which is characterized by the disappearance of long-range order of molecular orientation.

3. The behavior of the line width at the transition indicates the onset of easy diffusion, but T_1 up to the melting point is controlled largely by the jump rate for molecular reorientation.

4. The gradual increase of T_1 with temperature, above the transition, is caused primarily by an increase in the fraction of the total number of molecules for which reorientation is possible, rather than by temperature dependence of the jump rate for reorientation.

5. Reorientation does not always occur in the phase above the transition, but requires a minimum free volume. The temperature-independent T_1 observed in this phase under 1000 kg/cm^2 pressure is attributed to motions other than general reorientation.

A problem which had to be solved before the preceding NMR measurements were made was to prepare a dismountable pressure vessel seal which would function over a wide range of temperatures. "O" rings have a sizeable thermal expansion coefficient, and ultimately fail to seal at low temperatures. An unsupported-area seal utilizing Teflon was satisfactory. Provided that pressure is maintained during cooling, the Teflon flows sufficiently to maintain a seal at temperatures at least as low as -100°C, with nitrogen as the pressure fluid. This arrangement was carried over to the polyisobutylene work described in Sec. 1.

14. Spin-Lattice Relaxation Time in Ionic Crystals at Elevated Temperatures

(Reference: "Nuclear Magnetic Relaxation in Ionic Crystals at Elevated Temperatures" (Abstract), P. P. Mahendroo and A. W. Nolle, Bull. Am. Phys. Soc. II 5, 111 (1960).)

The preceding investigation of molecular motion in solids was extended by taking up the measurement of NMR relaxation times for the various nuclei in ionic crystals. NaCl, NaF, BaF_2, and LiF have been investigated from room temperature to 500°C or more.

Experimentally, the work is done by placing the sample and a surrounding r-f coil inside a solid copper jacket, wrapped with thin asbestos, the assembly fitting within the 1.25" gap of a permanent magnet. A noninductive electric heater is wound on a projecting copper rod, having a deep spiral groove, which is an integral part of the jacket. The nuclear magnetization is indicated by the amplitude of the "decay tail" (free induction voltage) following a "90° pulse". Magnetization measurements are made after selected growth times following an initial demagnetized state of the sample, obtained by applying 90° pulses in rapid succession.

The magnetic relaxation of the quadrupolar nuclei (Na^{23}, Li^7, etc.) is attributable to very high frequency fluctuations in the electric field gradients, which result in transfer of nuclear energy through Raman processes. Phonons of very high frequency may produce this result, as Van Kranendonk showed, or the optical lattice modes may do so by producing time-varying dipole moments, as other investigators have showed. The new experimental data are useful in searching for the limits of the Van Kranendonk temperature dependence, the form of which is, $T_1 = C_1 + C_2 T^{-2}$, T being absolute temperature. The data for Na^{23} in NaCl obey this

relationship well to at least 435°C, but the results for Na^{23} in NaF thus far obtained show disagreement above 200°C.

The magnetic relaxation of non-quadrupolar nuclei (F^{19}, in the present work) in ionic crystals permits identification of several other relaxation mechanisms, particularly, diffusion of positive ions (positive ion vacancies), diffusion of spin orientation to paramagnetic impurities, and paramagnetic relaxation as coupled to the relaxation of nuclear magnetic neighbors. The results for F^{19} in NaF above 300°C have been found to give an activation energy of 0.65 ev, which is consistent with positive ion diffusion. Diffusion is similarly identified in BaF_2 above 390°C, from T_1 data. A temperature independent T_1 for F^{19} in NaF for a range below 300°C is attributed tentatively to spin diffusion.

Extraordinarily long relaxation times (by comparison to values in other substances for this range of temperatures) are found in fluorine salts. For example, Fig. 14 shows T_1 vs. temperature for F^{19} in LiF, the value at room temperature being above 2000 sec. This feature makes these measurements so time consuming as to discourage many potentially interesting experiments on the effects of quenching or annealing.

E. Special Topics in Apparatus and Methods

15. Marginal Oscillator NMR Detector with Frequency Control

(Reference: "Automatic Frequency Control for a Marginal-Oscillator Magnetic Absorption Spectrometer", A. W. Nolle and H. L. Henneke, Rev. Sci. Instr. 28, 930 (1957).)

The usual marginal oscillator spectrometer (the Pound-Knight-Watkins instrument or instruments closely related to it) operates at the frequency of resonance of a tuned circuit which includes the sample-containing coil. In experiments with variable pressure or temperature, changes in the resonant circuit cause the spectrometer to operate at varying frequency. The modification which has been devised serves to reduce the frequency variations by a factor of the order of 10. The modification consists of adding a heterodyne stage, a low frequency discriminator, and a saturable reactor attached to the oscillator stage. These elements together form the frequency control loop. The system is advantageous in its ability to work over a wide range of oscillator voltages. In an application where this feature is not needed, it is simpler to stabilize the spectrometer frequency by injecting a weak signal from a stable external oscillator. A complete diagram is given in the reference.

16. Apparatus for Longitudinal Wave Transmission in High Polymers under Pressure

(See reference in Sec. 3.)

The experiment in question required that a laminar sample be inserted into the signal path of a pulse reflection apparatus, or removed, while the apparatus was inside a pressure vessel. This

requirement was solved with the bistable mechanical gate system sketched in section in Fig. 15. The total diameter of the assembly is approximately 1.5 in. The gate operates when the appropriate magnet winding is energized for about one second.

17. Spin-Echo Pulsing Equipment

The most elegant method of deriving controlled time intervals for spin-echo NMR experiments is to use sets of scalers actuated by a stable oscillator. For most of the work which has been reported here, however, sets of univibrators ("flip-flop" circuits) have been sufficient. These unistable devices, which are described in almost all books on electronic circuits, are basically two-tube circuits. For present purposes, however, a version using three triodes has been used. The third triode is used for triggering. This allows triggering to be accomplished by pulses having a wide range of rise times, without imposing any sizeable load on the basic two-tube circuit, and also permits wide latitude in the impedance of the driving circuits. The circuit is shown in Fig. 16. The whole circuit is effectively a pulse generator which is triggered by an input at I, and which delivers a pulse or voltage pedestal having a duration nearly proportional to the product RC.

For transmitter "keying" in spin echo work, amplified pulses are used from circuits of this kind in which the minimum RC is relatively small, so that pulse lengths of about 5 to 100 microsec are obtainable through adjustment of R. Time delay units are constructed by using the same circuit, but with values of RC available to permit pulse lengths from about 1 millisec to more

than 1 sec. The output is differentiated with a small capacitor, so that at the end of the delay interval a "pip" is available to trigger the transmitter pulse generator. Circuits for brightening the oscilloscope trace, at a selected time after the transmitter is operated, can be made up by cascading two of the circuits. one controls the time delay between an initiating event and the beginning of the brightening interval. The second controls the brightening duration. The output voltage of the brightening duration circuit is coupled directly to the grid-cathode circuit of the CRO tube, without differentiation, to serve as the brightening signal.

The particular time delay circuit which determined the spacing between the successive exposures, when used in making multiple-exposure spin-echo oscillograms, was in all cases fitted with step switches by which R could be increased in equal increments. Thus, the oscillograms were always made with equal time intervals between the exposures. In the interpretation of such an oscillogram, T_1 or T_2 is obtained as, say, "10.7 delay units". Then, with the help of a pair of dividers, 10.7 delay units is translated into actual time by reference to a timing wave of known frequency, which is always included in the photograph.

Where it was desired to combine the outputs of two or more delay circuits to trigger a single pulse generator, it proved helpful to have a "pip" generator thyratron circuit at the output of each delay generator. The "pip" generator thyratron discharges a 270 mmf capacitor through a 1000 ohm resistor, the voltage across the latter constituting the "pip". The outputs of these units may be switched together, through small capacitors, with no effect on the

delay generators which drive the pip generators.

18. Equipment for Direct Measurement of T_1

As indicated by the preceding section, NMR relaxation measurements by transient techniques have been most often carried out by multiple exposure photographic techniques, or by multiple observations, leading to plots of the time behavior of the amplitude of certain induced voltages due to nuclear magnetism. Where the plots are simple exponential decay or growth curves, relaxation times are unambiguously defined. Some curves which are not simple exponentials are expressible as the sum of two simple exponentials, corresponding to two relaxation times, and so forth. In still other cases, as when severe diffusion effects are present, no simple exponential fit is possible. Because of these complications, it is desirable to obtain the complete time plot of amplitude when an unfamiliar system is examined. Nevertheless, this is an unnecessary waste of time once it is established that a simple exponential function will be found. For use in cases where this is known to be true, a direct-reading system for measuring T_1 has been devised, as explained below.

The primary time standard is a stable audio oscillator, the frequency calibration of which is good to one per cent or better. As shown in the block diagram of Fig. 17, this drives a scaler, the final stage of which delivers a square wave having a period 64 times that of the oscillator. This square wave supplies the plate voltage for a thyratran "pip" generator of the type described in the preceding section, which is excited at the grid by the sine wave from the audio oscillator. The resulting voltage

pips, which are generated in active intervals of 32 oscillations of the primary generator, separated by equal inactive intervals, actuate the pulse generator associated with the transmitter (the pulsed r-f power source). The pips also initiate sweeps of an oscilloscope, which has a persistent screen.

In the simplest application, the Y deflection of the oscilloscope shows the voltage induced by free precession of the spins following the pulses. The oscilloscope shows a raster of 32 "decay tails" of generally decreasing amplitude for each active interval. The observer watches the first two of these. The first represents magnetization attained after effectively infinite waiting time. The second represents magnetization recovered after one period of the primary oscillator, provided that 90° pulses are used. The operator adjusts the oscillator frequency so that these have the ratio $(1 - e)$. Then T_1 is equal to the oscillator period.

This kind of direct setting of course demands that the operator see a display often enough to be able to make the timing adjustment conveniently. The arrangement is therefore most attractive for T_1 values of 0.2 sec or less. This range happens to be the one in which solutions of paramagnetic ions are conveniently studied.

With a slight modification, this equipment is useful in working with longer relaxation times. The "pip" generator is revised to become free-running. During the active interval of the equipment, which is still 32 periods of the basic oscillator, the transmitter delivers of the order of 1000 pulses/sec. As a

consequence, the sample is substantially demagnetized at the end of the active interval. The first free induction signal in the group produced in the next active interval indicates the amount of magnetization recovered during 32 periods of the basic oscillator. The use of various elapsed times gives data for a growth curve. If T_1 is no greater than a second or two, a direct-setting method based on finding a specified ratio of magnetization values is not inconvenient.

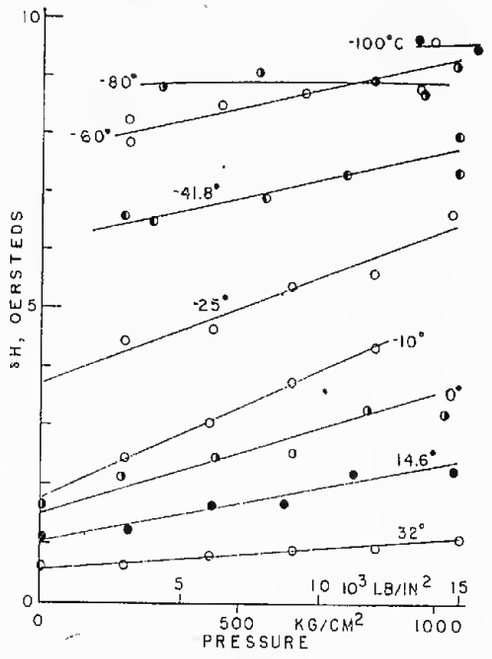

Fig. 1. Maximum-slope line width for proton magnetic resonance absorption in polyisobutylene, as a function of pressure, for various temperatures.

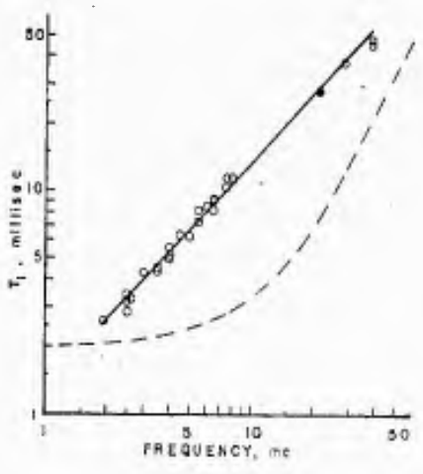

Fig. 2. Longitudinal NMR relaxation time for polyisobutylene as a function of frequency, at approximately 26°C. The result shown by the filled circle is due to Powles. The solid line corresponds to the first power of frequency. The broken curve is calculated from the theory of Bloembergen, Purcell, and Pound for a single relaxation time of 4×10^{-9} sec.

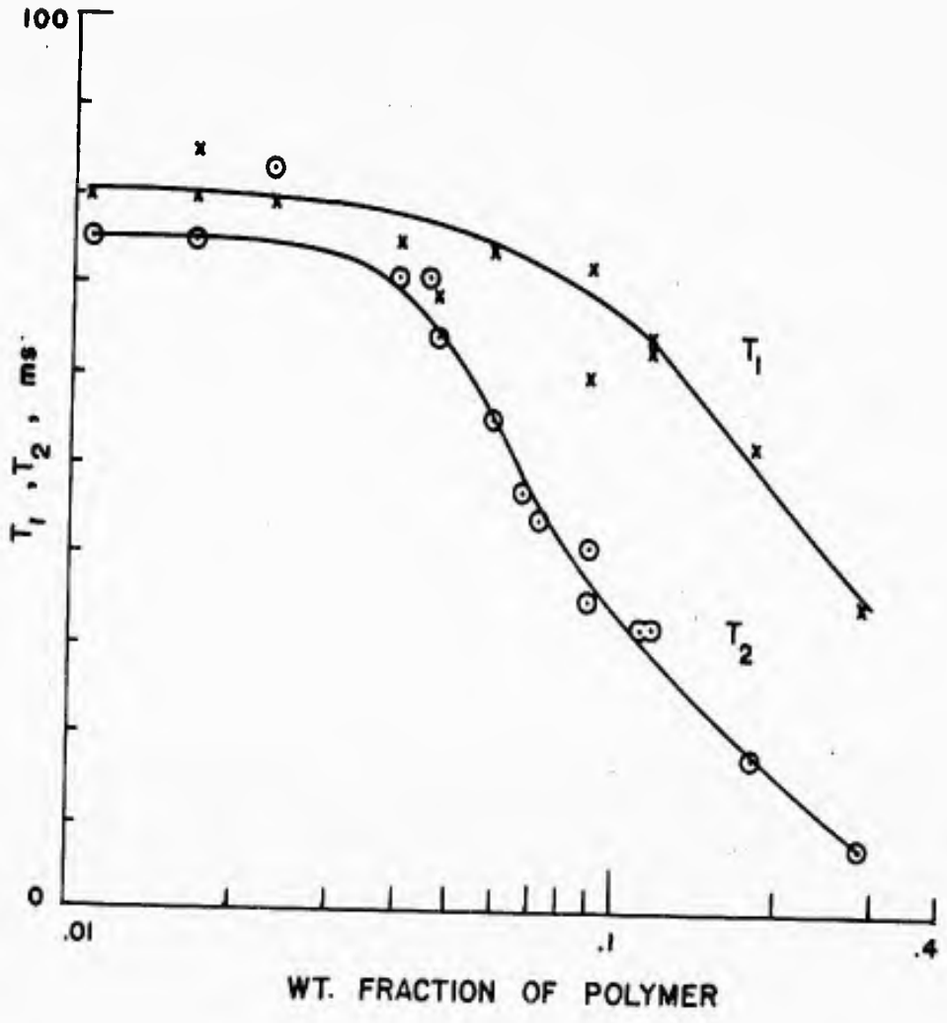

Fig. 3. Hydrogen nuclear magnetic resonance relaxation times at 25°C, as functions of weight fraction of polymer, for CCl_4 solutions of polyisobutylene of molecular weight 1.35×10^6.

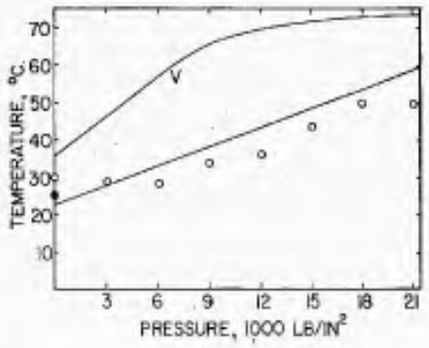

Fig. 4. Temperatures of maximum longitudinal-wave absorption in polyisobutylene at various constant pressures. Frequency, 4 mc. The straight line is not drawn to fit the data, but has the slope calculated by adapting a theory due to F. Bueche. The curve V is a constant-volume contour, for comparison. The filled circle shows a measurement given by Marvin, Aldrich, and Sack.

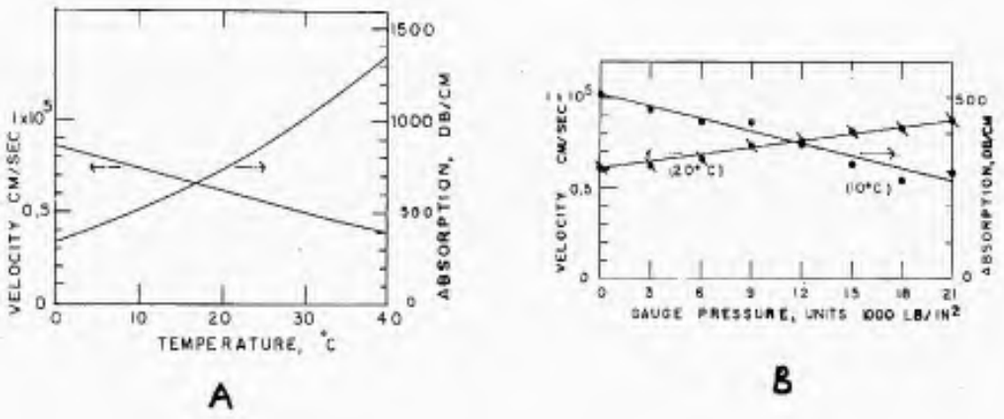

Fig. 5. Left: Phase velocity and absorption for 2 mc shear waves in polyisobutylene, computed from FGF reduced data for shear compliance. Right: Effects of pressure on these quantities, from present measurements.

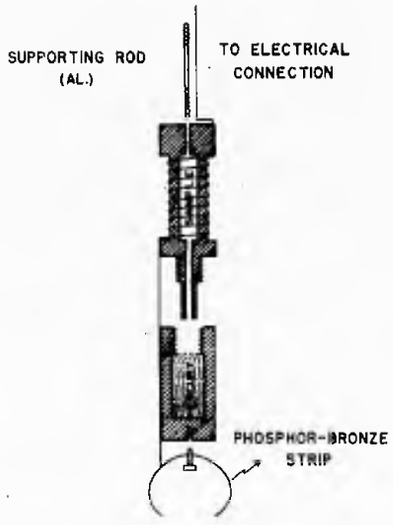

Fig. 6. Section of parts of cartridge of Kel-F plastic used in the measurement of the NMR spin-lattice relaxation time in degassed liquids under pressure.

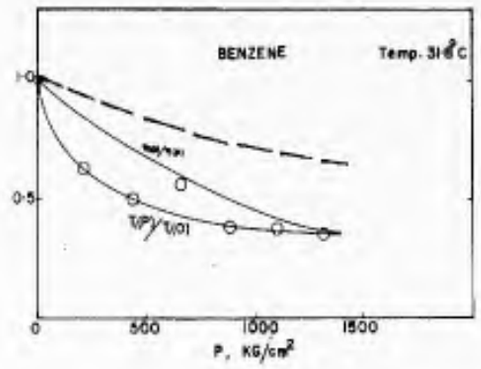

Fig. 7. Behavior of the inverse viscosity (fluidity) of benzene under pressure, and behavior of the NMR spin-lattice relaxation time in degassed and not-degassed samples (the latter shown by broken curve). The data are normalized to values at atmospheric pressure.

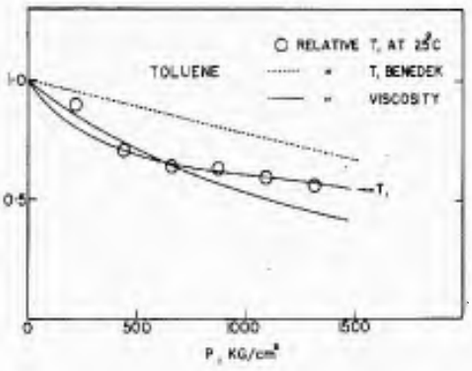

Fig. 8. Behavior of the inverse viscosity of toluene under pressure, and behavior of the NMR spin-lattice relaxation time in a degassed sample. Data normalized to values at one atmosphere. Results of Benedek and Purcell for a sample not degassed are also shown.

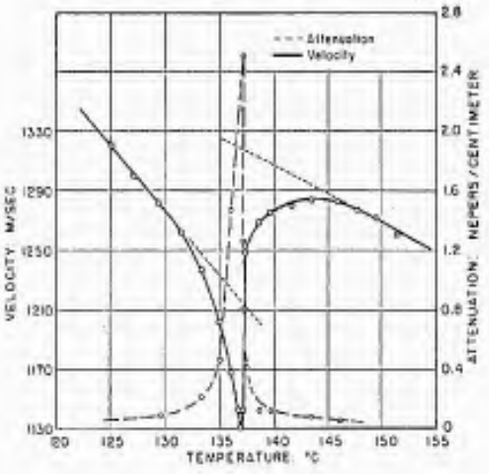

Fig. 9. Velocity and attenuation of 2 mc ultrasonic waves in p-azoxyanisole in the liquid-crystal transition region.

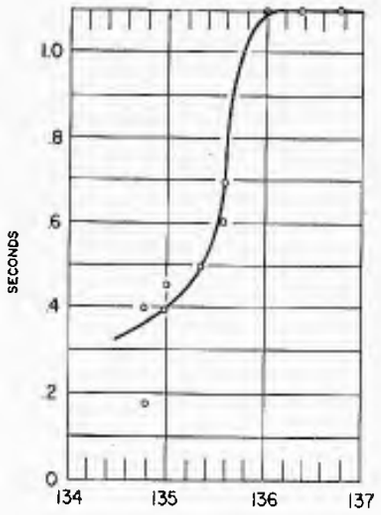

Fig. 10. Spin-lattice relaxation time vs. temperature in °C for hydrogen NMR in the isotropic phase of p-azoxyanisole at 28.8 mc, as the temperature is decreased by small steps toward the transition. At 135.5°, half the sample had gone into the anisotropic phase.

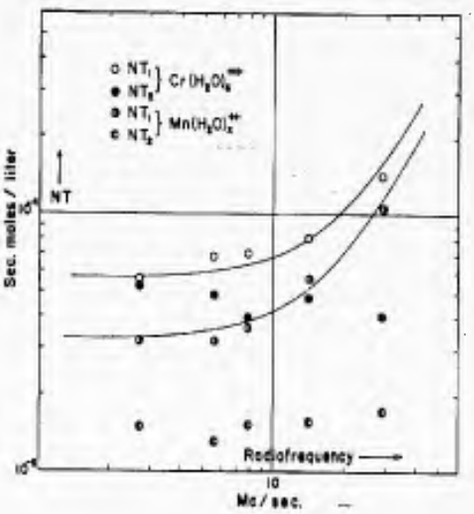

Fig. 11. The products NT_1 and NT_2 (relaxation times for unit concentration) as functions of experimental frequency, for hydrogen nuclear magnetic resonance in chromium and manganese solutions. The points are experimental; the curves are obtained by adjusting two constants in the theory for a single relaxation time.

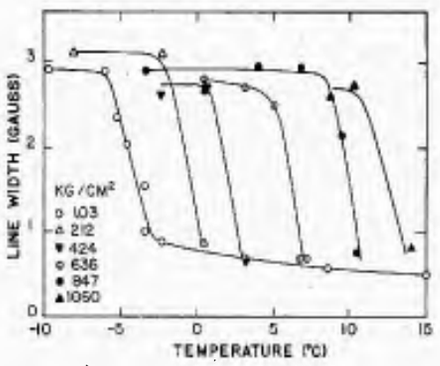

Fig. 12. NMR absorption line width for 2,2-dinitropropane.

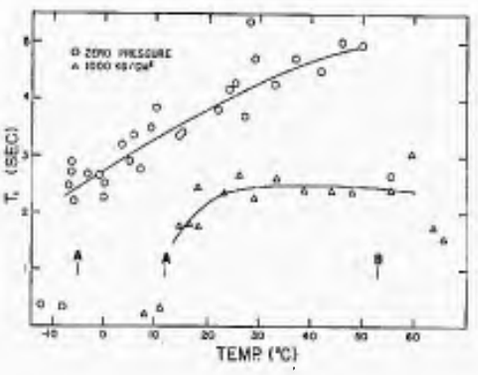

Fig. 13. Proton spin-lattice relaxation time for 2,2-dinitropropane at gauge pressures of zero and 1000 kg/cm². Points A are phase transition temperatures for the two pressures. Point B is the melting point at atmospheric pressure.

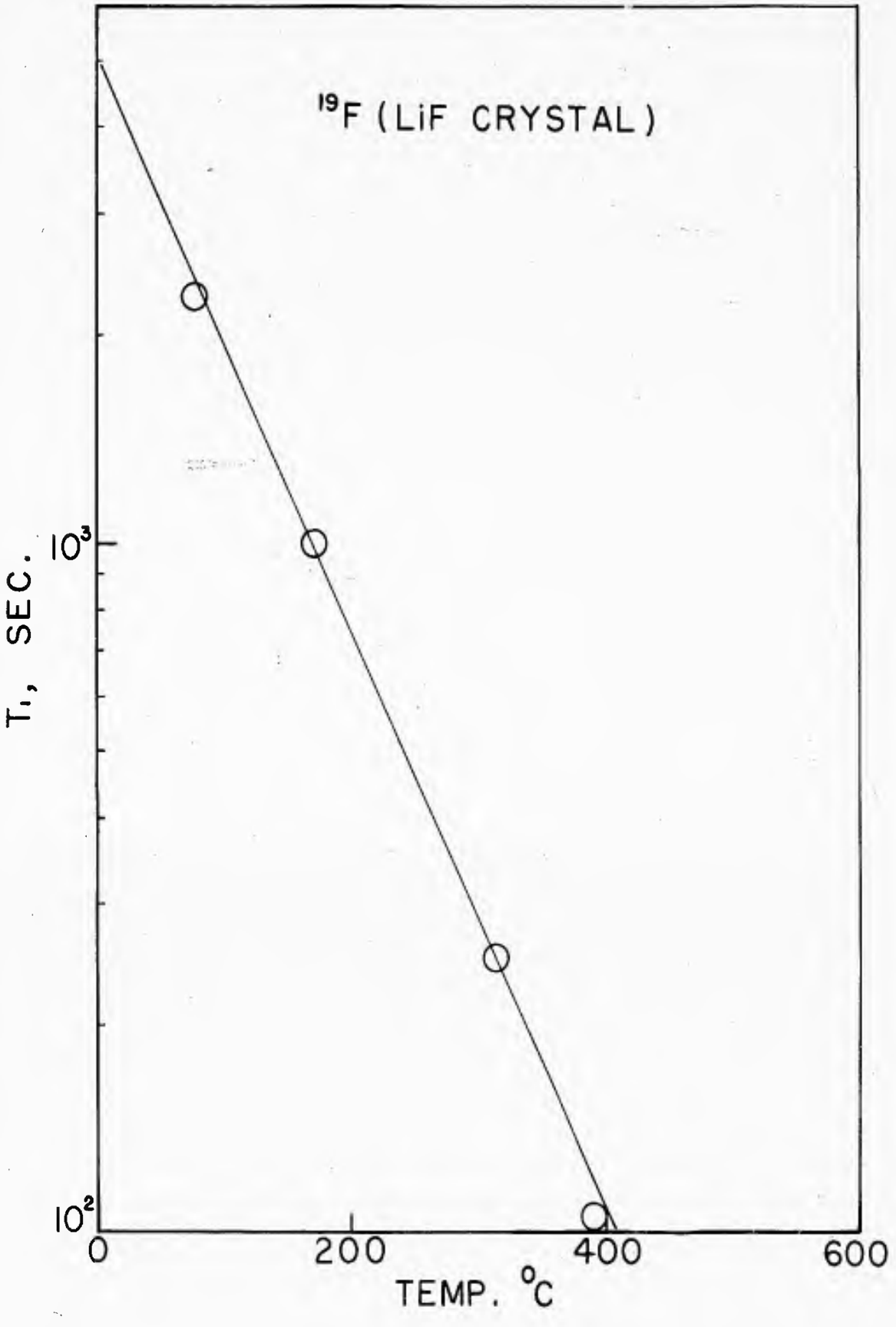

Fig. 14. Spin-lattice relaxation time for F^{19} in LiF as a function of temperature.

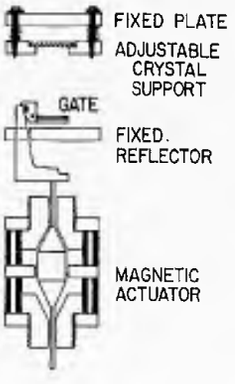

Fig. 15. Sectional sketch of magnetically actuated, bistable mechanical gate used to insert a laminar sample into the ultrasonic path in liquid inside a pressure vessel.

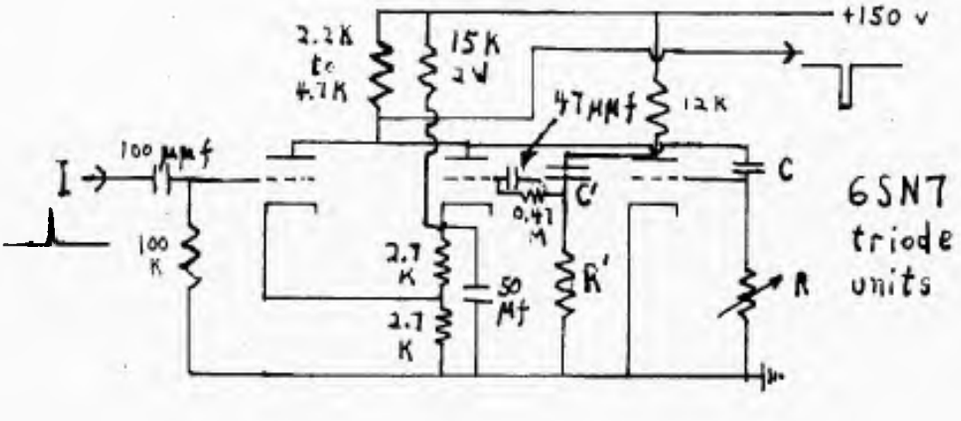

Fig. 16. Basic univibrator circuit used for making time delay units and pulse length control circuits. Output pulse width is of the order of RC. R'C' is considerably larger than RC. The elements between the junction of R', C' and the grid are omitted if required pulse lengths are not greater than a few millisec.

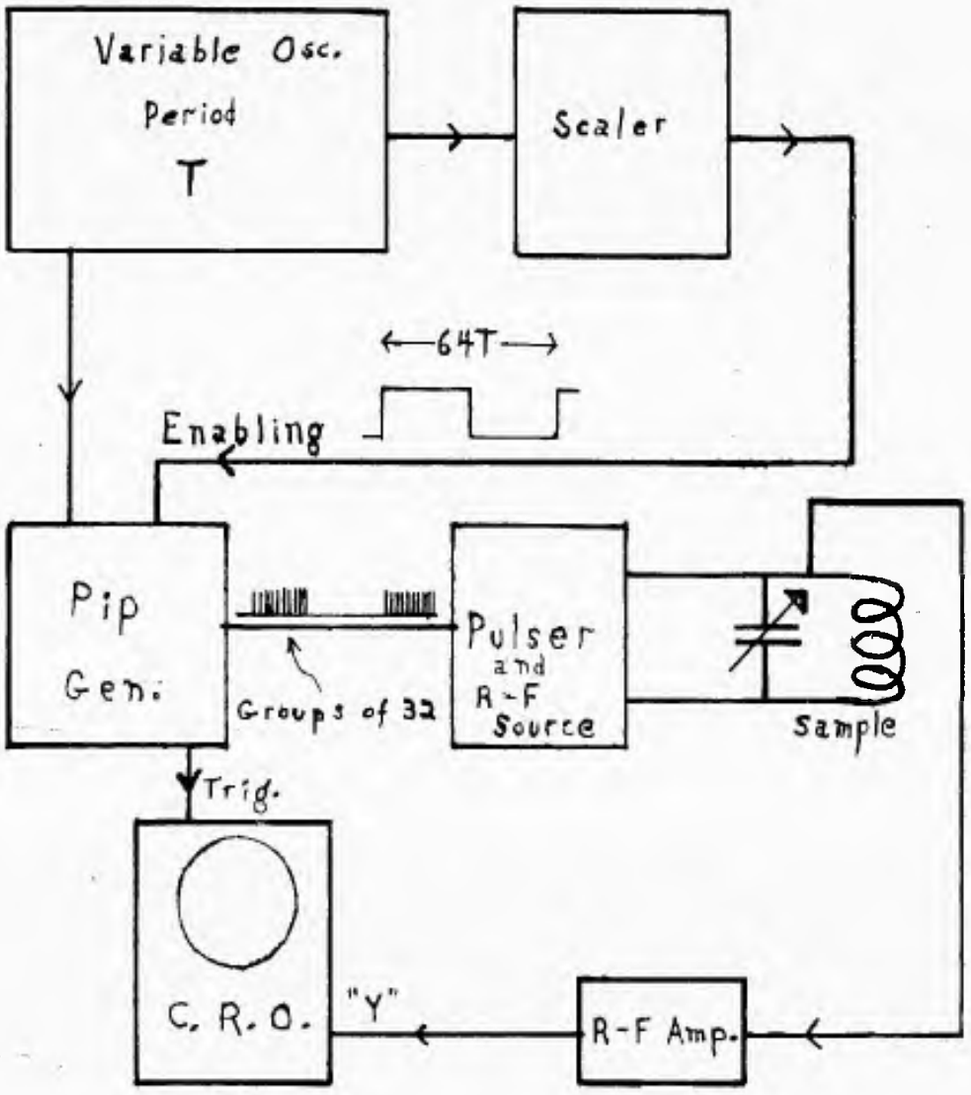

Fig. 17. Block diagram of apparatus for direct reading of spin-lattice relaxation time.

FINAL REPORT DISTRIBUTION LIST

THE UNIVERSITY OF TEXAS

Contract Nonr-375(05) NR NO 051-381

	No. Copies
Commanding Officer Office of Naval Research Branch Office The John Crerar Library Building 86 East Randolph Street Chicago 1, Illinois	(1)
Commanding Officer Office of Naval Research Branch Office 346 Broadway New York 13, New York	(1)
Commanding Officer Office of Naval Research Branch Office 1030 E. Green Street Pasadena 1, California	(1)
Commanding Officer Office of Naval Research Branch Office Navy #100 Fleet Post Office New York, New York	(7)
Director, Naval Research Laboratory Washington 25, D. C. Attn: Technical Information Officer Chemistry Division	(6) (2)
Chief of Naval Research Department of the Navy Washington 25, D. C. Attn: Code 425	(2)
Technical Library OASD (R&E) Pentagon Room 3E1065 Washington 25, D. C.	(1)
Technical Director Research & Engineering Division Office of the Quartermaster General Department of the Army Washington 25, D. C.	(1)
Research Director Chemical & Plastics Division Quartermaster Research & Engineering Command Natick, Massachusetts	(1)
Air Force Office of Scientific Research(SRLT) Washington 25, D. C.	(1)
Commanding Officer Diamond Ordnance Fuze Laboratories Washington 25, D. C. Attn: Technical Reference Section (ORDTL 06.33)	(1)
Office of Chief of Staff (R&D) Department of the Army Pentagon 3B516 Washington 25, D. C. Attn: Chemical Adviser	(1)
Chief, Bureau of Ships Department of the Navy Washington 25, D. C. Attn: Code 340	(2)
Chief, Bureau of Naval Weapons Department of the Navy Washington 25, D. C. Attn: Technical Library	(4)
ASTIA Document Service Center Arlington Hall Station Arlington 12, Virginia	(10)
Director of Research Signal Corps Engineering Laboratories Fort Monmouth, New Jersey	(1)
Naval Radiological Defense Laboratory San Francisco 24, California Attn: Technical Library	(1)
Naval Ordnance Test Station China Lake, California Attn: Head, Chemistry Division Code 40 Code 50	(1) (1) (1)

FINAL REPORT DISTRIBUTION LIST

THE UNIVERSITY OF TEXAS

Contract Nonr-375(05) NR NO 051-381

	No. Copies
Commanding Officer Office of Ordnance Research Box CM, Duke Station Durham, North Carolina	(1)
Brookhaven National Laboratory Chemistry Division Upton, New York	(1)
Atomic Energy Commission Research Division, Chemistry Branch Washington 25, D. C.	(1)
Atomic Energy Commission Library Branch Technical Information ORE Post Office Box E Oak Ridge, Tennessee	(1)
U.S. Army Chemical Warfare Laboratories Technical Library Army Chemical Center, Maryland	(1)
Office of Technical Services Department of Commerce Washington 25, D. C.	(1)
Dr. Albert Lightbody Naval Ordnance Laboratory White Oak, Silver Spring, Md.	(1)
Dr. W. H. Avery Applied Physics Laboratory The Johns Hopkins University 8621 Georgia Avenue Silver Spring, Maryland	(1)
Director, National Bureau of Standards Washington 25, D. C. Attn: Chief, Organic and Fibrous Materials Division	(1)
National Advisory Committee for Aeronautics 1512 H. Street N.W. Washington 25, D. C.	(1)
Chief, Bureau of Yards and Docks Department of the Navy Washington 25, D. C. Attn: Code P300	(1)
Commanding General Wright-Air Development Division Wright-Patterson Air Force Base, Ohio Attn: Materials Laboratory	(1)
Office of Chief of Engineers Research and Development Division Department of the Army Gravelly Point Washington 25, D. C.	(1)
Engineer Research & Dev. Lab. Fort Belvoir, Virginia Attn: Materials Branch	(1)
Commander Mare Island Naval Shipyard Rubber Laboratory Vallejo, California	(1)
Dr. J. H. Faull, Jr. 72 Fresh Pond Lane Cambridge 38, Massachusetts	(1)
Dr. R. S. Stein Department of Chemistry University of Massachusetts Amherst, Massachusetts	(1)
Dr. L. F. Rahm Plastics Laboratory Princeton University Princeton, New Jersey	(1)
Dr. A. V. Tobolsky Department of Chemistry Princeton University Princeton, New Jersey	(1)
Dr. R. M. Fuoss Department of Chemistry Yale University New Haven, Connecticut	(1)
Dr. W. Heller Department of Chemistry Wayne State University Detroit, Michigan	(1)

FINAL REPORT DISTRIBUTION LIST

THE UNIVERSITY OF TEXAS

Contract Nonr-375(05) NR NO. 051-381

	No. Copies	No. Copies
Dr. U. P. Strauss Department of Chemistry Rutgers University New Brunswick, New Jersey	(1)	
ONR Resident Representative University of Texas P. O. Box 7786 Austin, Texas	(1)	
Dr. H. S. Gutowsky Department of Chemistry University of Illinois Urbana, Illinois		
Commanding Officer Naval Air Development Center Johnsville, Pennsylvania Attn: Dr. Howard R. Moore	(1)	
Mr. J. B. Rust Hughes Aircraft Company Culver City, California		
Dr. Maurice Morton Institute of Rubber Research University of Akron Akron, Ohio	(1)	
Dr. G. Barth-Wehrenalp Pennsalt Cehmicals Corporation Box 4388 Philadelphia 18, Pennsylvania	(2)	
Dr. E. Grunwald Department of Chemistry Florida State University Tallahassee, Florida	(1)	